

PACS numbers: 42.62.Be; 87.63.lt; 87.64.mk; 87.57.Q–
DOI: 10.1070/QE2014v044n07ABEH015488

Comparison of *in vivo* and *ex vivo* laser scanning microscopy and multiphoton tomography application for human and porcine skin imaging

M.E. Darvin, H. Richter, Y.J. Zhu, M.C. Meinke, F. Knorr, S.A. Gonchukov, K. Köenig, J. Lademann

Abstract. **Two state-of-the-art microscopic optical methods, namely, confocal laser scanning microscopy in the fluorescence and reflectance regimes and multiphoton tomography in the autofluorescence and second harmonic generation regimes, are compared for porcine skin *ex vivo* and healthy human skin *in vivo*. All skin layers such as stratum corneum (SC), stratum spinosum (SS), stratum basale (SB), papillary dermis (PD) and reticular dermis (RD) as well as transition zones between these skin layers are measured noninvasively at a high resolution, using the above mentioned microscopic methods. In the case of confocal laser scanning microscopy (CLSM), measurements in the fluorescence regime were performed by using a fluorescent dye whose topical application on the surface is well suited for the investigation of superficial SC and characterisation of the skin barrier function. For investigations of deeply located skin layers, such as SS, SB and PD, the fluorescent dye must be injected into the skin, which markedly limits fluorescence measurements using CLSM. In the case of reflection CLSM measurements, the obtained results can be compared to the results of multiphoton tomography (MPT) for all skin layers excluding RD. CLSM cannot distinguish between dermal collagen and elastin measuring their superposition in the RD. By using MPT, it is possible to analyse the collagen and elastin structures separately, which is important for the investigation of anti-aging processes. The resolution of MPT is superior to CLSM. The advantages and limitations of both methods are discussed and the differences and similarities between human and porcine skin are highlighted.**

Keywords: *dermatology, imaging of human and porcine skin, confocal laser scanning microscopy, multiphoton tomography.*

1. Introduction

Mammalian skin is a boundary organ between the organism and the environment and has an important physiological and social function. Skin protects the body from mechanical damage, water loss and penetration of foreign compounds such as hazardous substances and bacteria, thereby providing regulation and a barrier function [1, 2]. Skin aging is determined by genetic aspects and can be strongly accelerated by the influence of environmental factors, the most important of which are air pollutants [3, 4], heat [5] as well as UV [6, 7], IR [8, 9] and visible [10, 11] components of solar radiation, which are able to generate free radicals in skin. Subsequent oxidative stress conditions may be a reason for the development of skin diseases and premature skin aging. Traditionally, skin is evaluated visually by a dermatologist, possibly even using magnifying and illuminating dermascopes. In cosmetology, different human skin layers are evaluated for skin aging and inflammation processes. However, in the case of skin diseases, the diagnosis is equivocal and histological analyses of skin biopsies become necessary. Removal of biopsies remains a highly invasive procedure for patients and volunteers and should possibly be replaced by nonbiopsy-based techniques. Noninvasive techniques that are appropriated for the measurement of skin parameters are very important in this regard.

Due to their noninvasiveness, high imaging quality and sensitivities to different skin structures and chemical compositions, optical microscopic methods are very promising for application in dermatology to visualise superficial layers and deeply located skin structures. Their application is important in medicine for the diagnosis of skin diseases and monitoring of the therapy efficiency [12], and in cosmetology for the characterisation of diverse skin parameters, such as skin barrier function, dryness and oiliness, furrows and wrinkles, penetration of topically applied formulations, etc. [13]. Confocal laser scanning microscopy (CLSM) [14, 15], multiphoton tomography (MPT) [16, 17], optical coherence tomography (OCT) [18, 19] and Raman microscopy (RM) [20, 21], which are intensively used worldwide in the field of dermatology, can be mentioned in this regard. These techniques are subject to continuous progress, providing a better image quality, sensitivity to different compounds, measurement speed, etc.

The present paper provides a comparison between two high-end microscopic systems – CLSM working in fluorescence and reflection regimes and MPT working in autofluorescence and second harmonic generation regimes, – which image the horizontal sections of skin at a high resolution. The images of different skin layers, such as SC, SS, SB, PD and RD, as well as of transition zones between the above-mentioned layers, are presented. The advantages, shortcomings and limitations of these microscopic methods are summarised and discussed. Because porcine skin serves as an appropriated model of human skin [22] and is widely used for investigations in the field of dermatology and cosmetology [23], the com-

M.E. Darvin, H. Richter, M.C. Meinke, F. Knorr, J. Lademann Center of Experimental and Applied Cutaneous Physiology, Department of Dermatology, Venerology and Allergology, Charité–Universität Berlin, Germany; e-mail: max_darvin@mail.ru;
Y.J. Zhu Zhejiang Center of Experimental and Applied Cutaneous Physiology, Department of Dermatology, Venerology and Allergology, Charité– Universitätsmedizin Berlin, Germany; Zhejiang University of Science and Technology, Hangzhou, P.R.China;
S.A. Gonchukov National Research Nuclear University 'MEPhI', Kashirskoe shosse 31, 115409 Moscow, Russia;
e-mail: gonchukov@mephi.ru;
K. Köenig JenLab GmbH, Schillerstr. 1, 07745 Jena, Germany

Received 7 March 2014; revision received 22 April 2014
Kvantovaya Elektronika **44** (7) 646–651 (2014)
Submitted in English

parison of the above-mentioned microscopic techniques is performed for both human skin *in vivo* and porcine skin *ex vivo*.

2. Materials and methods

2.1. Research objects

The *in vivo* skin measurements were performed on the inner forearm of healthy human volunteers, who were instructed not to use any cosmetic products for at least 48 hours and not to take a bath or shower for at least 8 hours previous to the beginning of the measurements. The skin areas selected for the measurements were without hairs and any visible distortions and abnormalities.

The *ex vivo* measurements were performed on fresh porcine ear skin. Porcine ear skin was obtained on the day of sacrifice, cleaned with cold running water, dried using a paper towel and analysed immediately after hair removal without influence on the stratum corneum. The study was approved by the Ethics Committee of the Charité – Universitätsmedizin, Berlin.

2.2. Confocal laser scanning microscopy

The investigations were carried out using a commercially available confocal laser scanning microscope (VivaScope® 1500 Multilaser, Mavig, Germany), which combines reflectance with fluorescent confocal laser scanning microscopy, making an *in vivo* optical biopsy possible in real time. Three wavelengths of 488 nm (blue), 658 nm (red) and 785 nm (near-infrared) are available as sources of excitation. Three filter sets permit the detection of reflectance only, fluorescence only and both signals together for each excitation wavelength. In all filter settings, a pinhole attenuates the light from out-of-focus planes that results in the high resolution of CLSM: a lateral resolution of 0.5 to 1 μm and an axial resolution of 3 to 5 μm. The CLSM imaging is based on the detection of reflection and fluorescence of light from the examined skin section. The scanned area measures 500×500 μm, producing images of 1000×1000 pixels. Differences in the refractive indices of cell structures and skin layers show reflection patterns that are translated into grayscale to create the image. Images are analysed using customised VivaScope software. The maximum measuring depth into the skin can reach 300 μm for an excitation wavelength of 785 nm, but in fact it does not exceed 200 μm.

For making use of the fluorescence capabilities of CLSM, different fluorescence-active dyes should be injected intradermally under standardised conditions for the labelling of skin structures to achieve an appropriated contrast. Sodium fluorescein, methylene blue and indocyanine green are suitable fluorescence-active dyes suggested for application, using the excitation wavelengths at 488 nm, 658 nm and 785 nm, respectively. The SC could be analysed using topical application of the above- mentioned dyes. During the microscopic measurements, the laser focus is moved from the skin surface into deeper parts of the skin at different increments to reach deeply located dermal areas. A more detailed description of utilised CLSM has been published elsewhere [24, 25].

2.3. Multiphoton tomography

The investigations were carried out using a commercially available multiphoton tomograph (JenLab GmbH, Jena, Germany) equipped with a tunable femtosecond Ti : sapphire laser (Mai Tai XF, Spectra Physics, USA) and adapted for *in vivo* measurements. The tunable laser (710–920 nm) generated 100 fs pulses at a repetition rate of 80 MHz. To investigate the deeply located skin areas, the excitation wavelength of 760 nm was used, which provides high penetration ability due to the reduced absorption and scattering of skin. For studying the skin structure at different depths, sensitive photomultipliers were used for the detection of autofluorescence (AF) and second harmonic generation (SHG) signals simultaneously in two channels.

Collagen molecules are not centrosymmetric with an extremely high level of crystallinity that makes them exceptionally efficient in generating the SHG signal [26]. AF/SHG channels are important for the investigation of the dermis where the elastin concentration (AF intensity) and collagen concentration (SHG intensity) could be measured separately [26, 27]. Radiation collected from different depths was averaged over slices. In one scan, a maximum area of about 350×350 μm can be imaged. The applied power in the skin increased linearly with depth from 10 mW on the skin surface to a maximal allowed value of 50 mW, which is enough for obtaining the qualitative images in the dermis. The acquisition time was changed from 3 to 13 seconds for one slice depending on the measurement conditions. These parameters guaranteed satisfactory measurement stability and image quality. The highest two-photon absorption probability is achieved only in the focus of the optical system, thus providing a high resolution. The lateral and axial resolution was 0.5 and 2 μm, respectively. The maximum measuring depth into the skin was limited to 400 μm, but in fact did not exceed 150 μm.

The lifetime of AF, which varies for different cutaneous chromophores, can be measured at every image point using the fluorescence lifetime imaging (FLIM) technique. Typically for the skin, the fluorescence decay is characterised by the parameters of a biexponential approximation curve (quick and slow components) [28]. A more detailed description of the utilised MPT was previously presented by Konig et al. [28, 29].

3. Results

3.1. Examples of skin layer images

The images of such skin layers as SC, SS, SB, PD and RD obtained *in vivo* on healthy human skin using CLSM (in the fluorescence and reflectance modes) and MPT (in the AF and SHG modes) are presented in Fig. 1. Figure 2 shows the same skin layers obtained *ex vivo* on porcine ear skin. The SHG images of SC, SS and SB are not presented in Figs 1 and 2 because in these skin layers there is no SHG signal from collagen. The obtained picture quality is sufficient to clearly distinguish between different skin layers and to determine their thickness. Additionally, it was possible to evaluate corneocytes and their structure in the SC. Compartments of the epidermal cells in the SS (nucleus, cytoplasm, and intracellular area), papillary structure and blood capillaries in the PD, collagen and elastin fibres in the RD can be also well recognised. The obtained images are comparable to the histological images of human skin, which are shown in Fig. 3 for SC, SS and PD skin layers.

In the case of fluorescence measurements, the AF of cutaneous chromophores [keratin, NAD(P)H, flavin, etc.] can be

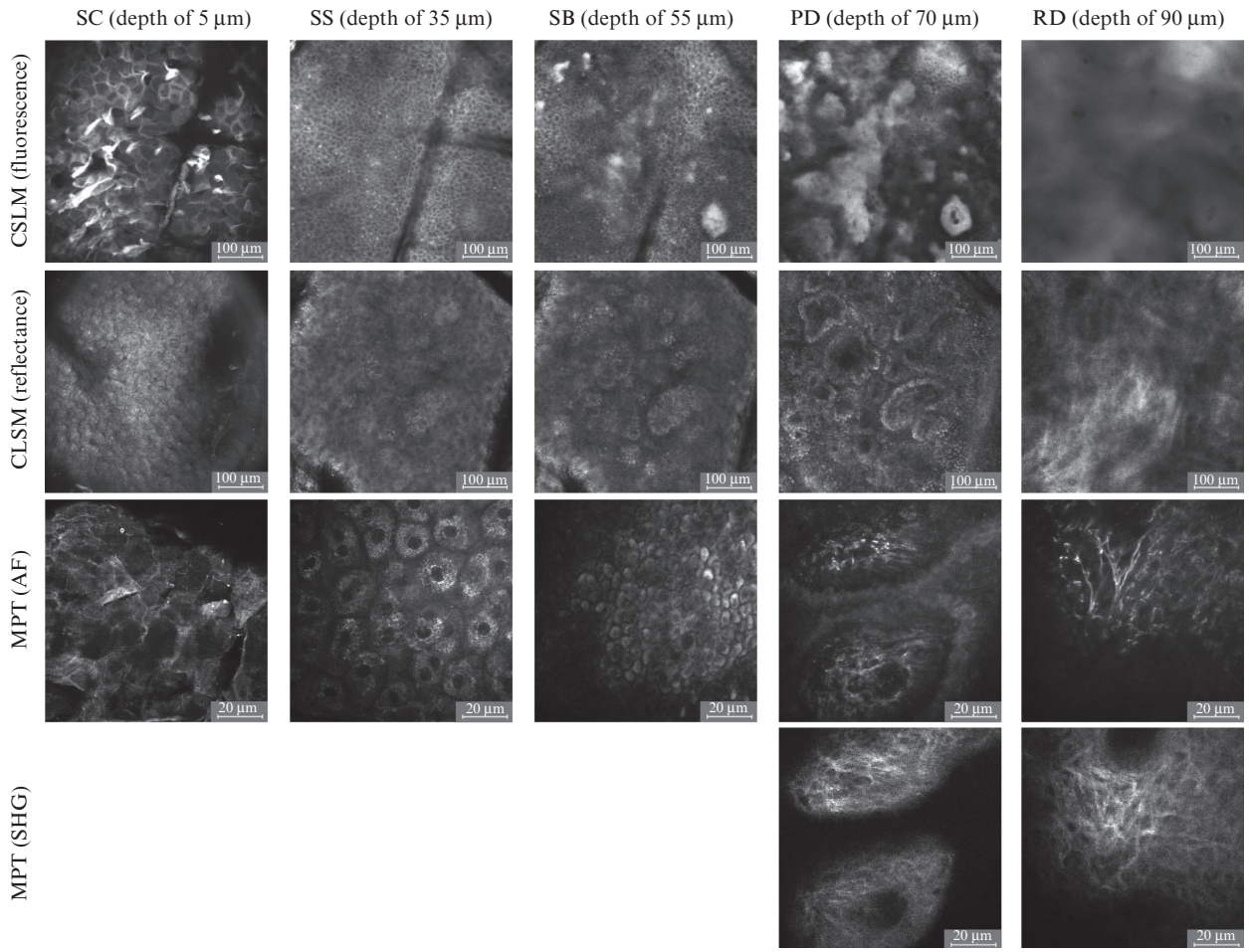

Figure 1. Images of different skin layers obtained *in vivo* on healthy human inner forearm skin samples by using CLSM (in the fluorescence and reflectance regimes) and MPT (in the AF and SHG regimes). All images obtained using CLSM (fluorescence regime) were measured under the excitation at 488 nm after the injection of sodium fluorescein. Images of SC, SS and SB skin layers obtained using CLSM (reflectance regime) were measured under the excitation at 488 nm, and of PD and RD skin layers under the excitation at 785 nm. MPT (both AF and SHG regimes) images were obtained under the excitation at 760 nm [the MPT (SHG regime) images of SC, SS and SB skin layers are not presented due to the absence of collagen in these skin layers]. The image size is 500×500 μm for CLSM (fluorescence and reflectance regimes) and 100×100 μm for MPT (AF and SHG regimes).

excited directly by MPT, while using CLSM, a fluorescent dye has to be applied in order to make the structure in different skin layers visible. A topically applied dye does not penetrate through the intact skin barrier efficiently, which allows only superficial SC layers to be investigated. Only if the dye is injected into the tissue, the upper layers of the skin can be detected as seen in Figs 1 and 2 (CLSM, fluorescent regime). The amount of injected dye must be measured exactly in order to obtain, on the one hand, a significant CLSM signal and to avoid, on the other hand, overloading with the dye, which would prevent the structure of the skin from being visualised. For this reason approximately 1 μL of the fluorescence dye was injected in the area between the epidermis and dermis (depth around 40 μm) using the syringe.

Using CLSM, the cellular structure can be much better detected in the fluorescence regime than in the reflectance one. The advantage of the latter is that the skin can be measured directly without an additional dye. Using the reflectance regime, the different layers up to a depth of approximately 150 μm can be easily analysed, excluding the upper SC layers. With a deeper penetration inside the skin up to the blood capillaries, it is even possible to detect the blood flow, however, only in the reflectance regime.

Using MPT, the structures of single cells and their compartments can be easily visualised by the AF intensity without external application of dyes. The intensity of laser photons in the focus is high so that SHG processes can be stimulated. Collagen generates an SHG signal and has low AF, while elastin, on the contrary, generates a high AF and has no SHG. The SHG-to-AF aging index of dermis (SAAID) has been developed for *ex vivo* and *in vivo* characterisation of skin aging processes [27, 30] and is used virtually for the *in vivo* analyses of the sunscreen efficiency with MPT [31]. These measurements are of high importance in cosmetology, because collagen can be classified as the hallmark of development of premature skin aging [32, 33] (see Figs 1 and 2, PD and RD skin layers). A similar image can also be obtained using the reflectance regime of CLMS, whereby the structure is strongly blurred, on account of the larger size of the focus. In this case, not only collagen but also elastin fibres are detected. Thus, CLSM cannot distinguish between collagen and elastin in the dermis, measuring only their total superposition, while MPT can distinguish between these two proteins.

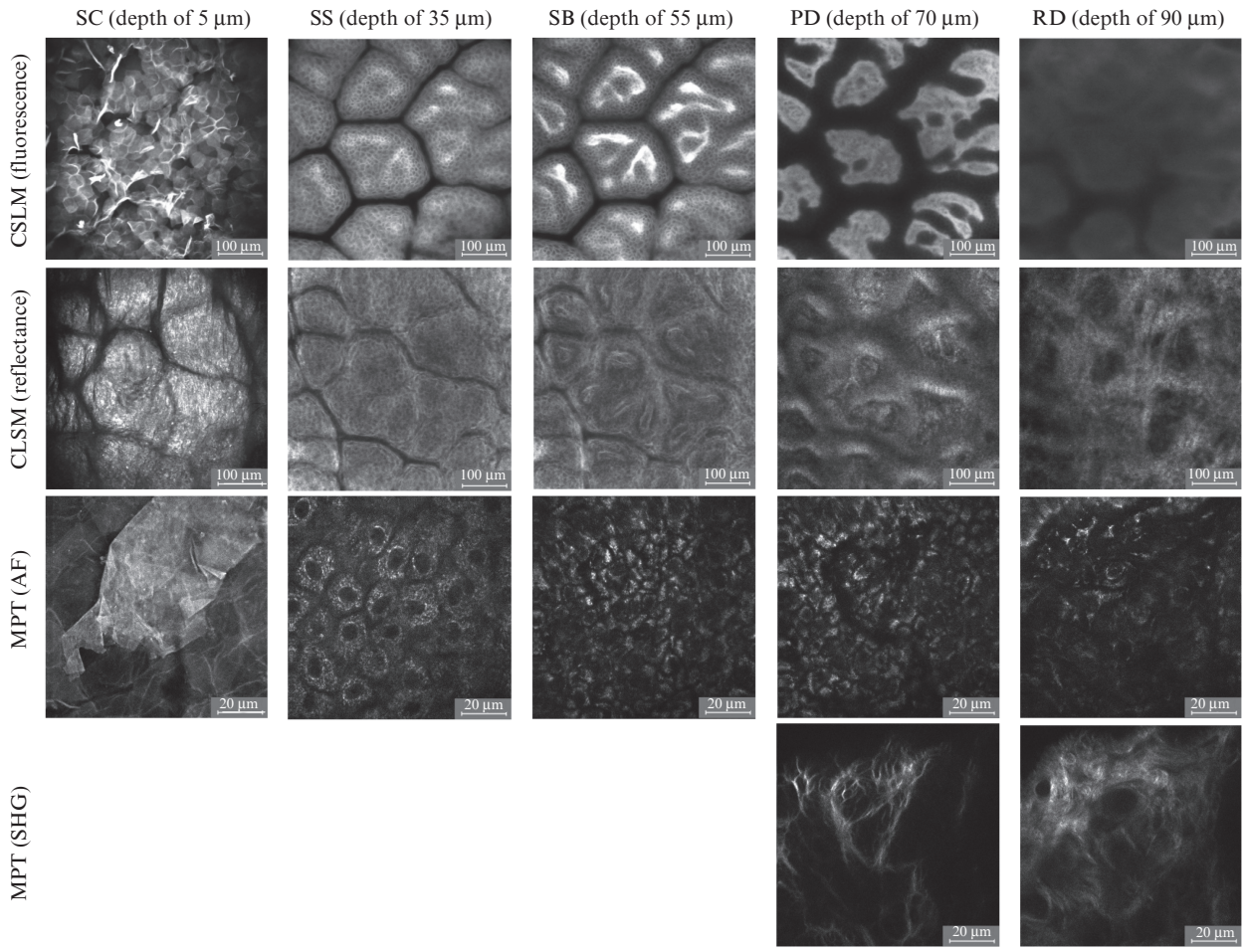

Figure 2. Images of different skin layers obtained *ex vivo* on porcine ear skin samples. Other notations are the same as in Fig. 1.

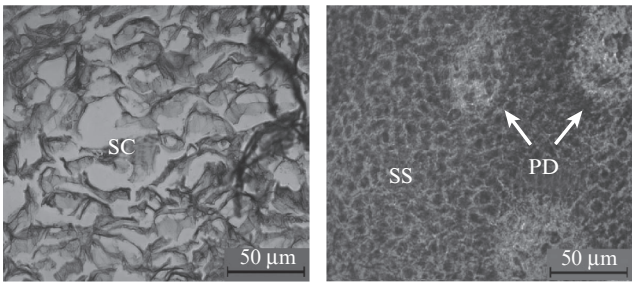

Figure 3. Histological sections of SC (depth of 0–5 μm), SS and PD (depth of 55–65 μm) layers of human skin [13].

The resolution of MPT is superior in comparison with the fluorescence and reflectance regimes of CLSM, which is achieved because of the small size of the focus of the laser excitation beam in the multiphoton absorption.

3.2. Similarities/differences between human and porcine skin

Comparison of the images of human and porcine skin showed that there are almost no differences in the corneocytes of the SC as well as in the form and density of SS cells. The shape and size of corneocytes and single cells are very similar. The parameters of SS, such as nucleus size, amount of cytoplasm and intracellular area, are fully identical in human and porcine skin. The only difference is the presence of 'small islands' of about 100–150 μm in porcine skin, which are invisible in human skin. The SB layer looks similar excluding the melanin distribution. In the PD layer, the papillary structure is more pronounced in human skin in the form of collagen rings, while in the case of porcine skin, collagen looks branchy and inhomogeneous. In the deeply located RD, elastin and collagen fibres cover all volumes and appear comparable to human and porcine skin.

4. Discussion

The described multi-laser CLSM, combining both reflectance and fluorescence regimes, is widely used clinically for the diagnosis of skin diseases and different types of skin cancer [14, 34]. However, for the fluorescence measurements, an exogenous dye must be applied. In the case of topical application, the dye accumulates on the skin surface and in the first upper SC layers. These measurements are well suited for the investigation of dry skin to obtain information about skin hydration. If layers deeper than the SC are investigated, usually sodium fluorescein, methylene blue or indocyanine green must be injected. This represents an invasive procedure, which cannot be utilised in all situations. Additionally, the application of a fluorescent dye has the disadvantage that it must be administered precisely, due to the fact that the dye is distributed in the tissue within a few minutes, so that afterwards only a continuous fluorescence background can be detected.

Nevertheless, the fluorescence measurements are well suited for the investigation of the distribution of topically applied formulations on the skin surface, such as sunscreens, and the analysis of the penetration of fluorescence-labelled substances in the skin barrier [35].

Using the reflectance regime of the CLSM system, only the skin layers underneath the SC could be analysed showing a weak resolution, as in the case of fluorescence measurements. In this case, dye application is not necessary. Reflectance measurements are well suited to analyse the deeper structure of the skin, such as melanin distribution, as illustrated in Figs 1 and 2 in the SB section for human and porcine skin. The melanin is visualised in the form light spots in the image. The amount of melanin can be quantified by an evaluation program provided by the Vivascope manufacturers. The analysis of elastin fibres is limited due to the fact that elastin and collagen cannot be distinguished using both CLSM regimes, which is necessary for the measurements in the field of skin aging.

Several of these limitations can be overcome using MPT measurements. The resolution of the obtained images is of a better quality than for CLSM. Cells, cell compartments, as well as distances between cells can be analysed in the AF regime. In the case of inflammatory processes, also inflammatory cells can be visualised in the SS. In the SB and PD, the melanin distribution and the structure of collagen and elastin fibres can be detected. Because of the continuous generation of AF, reflectance measurements cannot be performed by means of MPT. The intensity of the laser focus allows generating the SHG signal if the corresponding tissue is available. The collagen fibres are the SHG-active structures and visible in the PD and RD regions (see Figs 1 and 2).

Investigation of the penetration of cosmetic formulations inside skin using MPT can be performed in three different ways: by the AF intensity [36], by FLIM [37] and by SHG intensity, as was shown for SHG-active zinc oxide nanoparticles [16]. The shortcoming of the utilised MPT system lies in the impossibility to scan large skin areas, which can be solved by adding the advantages of OCT. The combination of MPT and OCT into a single platform was reported to be efficient for clinical diagnosis *in vivo*. Scanning of large skin regions using OCT helps to locate abnormal regions quickly, and the subsequent application of MPT on these regions gives microscopic information at sub-cellular resolution [38].

The distribution of water and lipids in skin can be additionally measured using MPT combined with the CARS system [39, 40]. Information about the lipids could give an advantage in analysing different skin diseases and subsequent therapy control [40, 41]. Both water and lipid distributions could present a potential for the cosmetic industry by analysing 'oil in water' or 'water in oil' composition of cosmetic formulations as well as their influence on skin.

CLSM and MPT are well suited for the *in vivo* and *ex vivo* investigations of the skin structure and the determination of the thickness of the skin layers. The image size and resolution obtained using both methods give an additional possibility to analyse the cutaneous macro-structures, such as furrows and wrinkles, sweat glands and orifices of hair follicles. Both CLSM and MPT methods can be used for monitoring wound healing processes [25, 42], for diagnostics of skin diseases [14, 29] and therapy control [24, 29]. Reflectance CLSM and MPT were recently compared for detection of basal cell carcinoma [17] and other skin diseases [43] in clinical use and were found to be appropriate for this task.

The other technique promising to be very effective for the *in vivo* measurement of penetration profiles of cosmetic formulations and for the diagnosis of skin diseases including skin cancer is Raman microscopy (RM) [44]. Utilisation of both fingerprint [45, 46] and high wavenumber [47] regions can be mentioned in this regard. RM does not provide high-resolution images, and the obtained spectra should be analysed. Probably, in the future, RM may also be effective for the diagnosis of skin diseases and therapy control.

5. Conclusions

In summarising the results of the two compared imaging systems, it could be well demonstrated that skin measurements for cosmetic applications can be successfully undertaken with MPT and only partly with CLSM. In the case of medical application of both systems, the main subject of microscopic investigations is the diagnosis and therapy control of skin diseases. In this respect, the reflectance regime of the CLSM systems is sufficient enough to obtain an efficient analysis. The high cost of MPT in comparison to that of CLSM presents another argument for more frequent utilisation of CLSM in skin research.

The comparison of the *ex vivo* and *in vivo* measurements, carried out on porcine ear skin and human skin, clearly demonstrates that both types of skin show the same structure. The results obtained in this study underline once again the fact that porcine ear skin is a suitable model for human skin.

As a result, it can be established that both systems, CLSM and MPT, have their advantages and limitations: An optimal system should be selected based on the results of the study.

Acknowledgements. This work was partially supported within the framework of the 'Biofeedback' Project (13N12593) by the German Ministry of Education and Research.

References

1. Norlen L. *Skin Pharmacol. Physiol*., **26**, 213 (2013).
2. Windbergs M., Hansen S., Schroeter A., Schaefer U.F., Lehr C.M., Bouwstra J. *Skin Pharmacol. Physiol*., **26**, 317 (2013).
3. Stone V., Johnston H., Clift M.J. *IEEE Trans. Nanobiosci*., **6**, 331 (2007).
4. Burke K.E., Wei H. *Toxicol. Ind. Health*, **25**, 219 (2009).
5. Akhalaya M.Y., Maksimov G.V., Rubin A.B., Lademann J., Darvin M.E. *Ageing Res. Rev.*, DOI: 10.1016/j.arr.2014.03.006 (2014).
6. Biniek K., Levi K., Dauskardt R.H. *Proc. Nat. Acad. Sci. U.S.A.*, **109**, 17111 (2012).
7. Poljsak B., Dahmane R. *Dermatol. Res. Pract*., **2012**, 135206 (2012).
8. Darvin M.E., Haag S., Meinke M., Zastrow L., Sterry W., Lademann J. *Skin Pharmacol. Physiol*., **23**, 40 (2010).
9. Darvin M.E., Haag S.F., Lademann J., Zastrow L., Sterry W., Meinke M.C. *J. Invest Dermatol*., **130**, 629 (2010).
10. Zastrow L., Groth N., Klein F., Kockott D., Lademann J., Renneberg R., Ferrero L. *Skin Pharmacol. Physiol.*, **22**, 31 (2009).
11. Liebel F., Kaur S., Ruvolo E., Kollias N., Southall M.D. *J. Invest. Dermatol*., **132**, 1901 (2012).
12. Drakaki E., Vergou T., Dessinioti C., Stratigos A.J., Salavastru C., Antoniou C. *J. Biomed. Opt*., **18**, 061221 (2013).
13. Lademann J., Patzelt A., Darvin M., Richter H., Antoniou C., Sterry W., Koch S. *Laser Phys. Lett*., **5**, 335 (2008).
14. Ulrich M., Lange-Asschenfeldt S. *J. Biomed. Opt.*, **18**, 061212 (2013).
15. Zhang L.W., Monteiro-Riviere N.A. *J. Biomed. Opt*., **18**, 061214 (2013).

16. Darvin M.E., Konig K., Kellner-Hoefer M., Breunig H.G., Werncke W., Meinke M.C., Patzelt A., Sterry W., Lademann J. *Skin Pharmacol. Physiol*., **25**, 219 (2012).
17. Ulrich M., Klemp M., Darvin M.E., Konig K., Lademann J., Meinke M.C. *J. Biomed. Opt*., **18**, 61229 (2013).
18. Sattler E., Kastle R., Welzel J. *J. Biomed. Opt*., **18**, 061224 (2013).
19. Greaves N.S., Benatar B., Whiteside S., Alonso-Rasgado T., Baguneid M., Bayat A. *Br. J. Dermatol*., **170** (4), 840 (2014).
20. Ali S.M., Bonnier F., Tfayli A., Lambkin H., Flynn K., McDonagh V., Healy C., Clive Lee T., Lyng F.M., Byrne H.J. *J. Biomed. Opt*., **18**, 061202 (2013).
21. Darvin M.E., Meinke M.C., Sterry W., Lademann J. *J. Biomed Opt*., **18**, 61230 (2013).
22. Debeer S., Le Luduec J.B., Kaiserlian D., Laurent P., Nicolas J.F., Dubois B., Kanitakis J. *Eur. J. Dermatol.*, **23**, 456 (2013).
23. Jacobi U., Kaiser M., Toll R., Mangelsdorf S., Audring H., Otberg N., Sterry W., Lademann J. *Skin Res. Technol*., **13**, 19 (2007).
24. Ulrich M., Krueger-Corcoran D., Roewert-Huber J., Sterry W., Stockfleth E., Astner S. *Dermatology,* **220**, 15 (2010).
25. Lange-Asschenfeldt S., Bob A., Terhorst D., Ulrich M., Fluhr J., Mendez G., Roewert-Huber H.J., Stockfleth E., Lange-Asschenfeldt B. *J. Biomed. Opt*., **17**, 076016 (2012).
26. Lin S.J., Wu R.J., Tan H.Y., Lo W., Lin W.C., Young T.H., Hsu C.J., Chen J.S., Jee S.H., Dong C.Y. *Opt. Lett*., **30**, 2275 (2005).
27. Breunig H.G., Studier H., Konig K. *Opt. Express*, **18**, 7857 (2010).
28. Konig K., Raphael A.P., Lin L., Grice J.E., Soyer H.P., Breunig H.G., Roberts M.S., Prow T.W. *Adv. Drug Delivery Rev.*, **63**, 388 (2011).
29. Konig K. *J. Biophotonics*, **1**, 13 (2008).
30. Kaatz M., Sturm A., Elsner P., Konig K., Buckle R., Koehler M.J. *Skin Res. Technol*., **16**, 131 (2010).
31. Darvin M.E., Richter H., Ahlberg S., Haag S.F., Meinke M.C., Le Quintrec D., Doucet O., Lademann J. *J. Biophotonics*, DOI: 10.1002/jbio.201300171 (2014).
32. Proksch E., Schunck M., Zague V., Segger D., Degwert J., Oesser S. *Skin Pharmacol. Physiol*., **27**, 113 (2014).
33. Proksch E., Segger D., Degwert J., Schunck M., Zague V., Oesser S. *Skin Pharmacol. Physiol*., **27**, 47 (2014).
34. Sattler E., Kastle R., Arens-Corell M., Welzel J. *Skin Res. Technol.*, **18**, 370 (2012).
35. Patzelt A., Lademann J., Richter H., Darvin M.E., Schanzer S., Thiede G., Sterry W., Vergou T., Hauser M. *Skin Res. Technol*., **18**, 364 (2012).
36. Vergou T., Patzelt A., Schanzer S., Meinke M.C., Weigmann H.J., Thiede G., Sterry W., Lademann J., Darvin M.E. *Skin Pharmacol. Physiol*., **26**, 30 (2013).
37. Leite-Silva V.R., Le Lamer M., Sanchez W.Y., Liu D.C., Sanchez W.H., Morrow I., Martin D., Silva H.D., Prow T.W., Grice J.E., Roberts M.S. *Eur. J. Pharm. Biopharm.*, **84**, 297 (2013).
38. Alex A., Weingast J., Weinigel M., Kellner-Hofer M., Nemecek R., Binder M., Pehamberger H., Konig K., Drexler W. *J. Biophotonics*, **6**, 352 (2013).
39. Konig K., Breunig H.G., Buckle R., Kellner-Hofer M., Weinigel M., Buttner E., Sterry W., Lademann J. *Laser Phys. Lett*., **8**, 465 (2011).
40. Breunig H.G., Weinigel M., Buckle R., Kellner-Hofer M., Lademann J., Darvin M.E., Sterry W., Konig K. *Laser Phys. Lett*., **10**, 025604 (2013).
41. Weinigel M., Breunig H.G., Kellner-Höfer M., Bückle R., Darvin M.E., Klemp M., Lademann J., König K. *Laser Phys. Lett*., **11**, 055601 (2014).
42. Deka G., Wu W.W., Kao F.J. *J. Biomed. Opt*., **18**, 061222 (2013).
43. Koehler M.J., Speicher M., Lange-Asschenfeldt S., Stockfleth E., Metz S., Elsner P., Kaatz M., Konig K. *Exp. Dermatol*., **20**, 589 (2011).
44. Schleusener J., Reble C., Helfmann J., Gersonde I., Cappius H.-J., Glanert M., Fluhr J.W., Meinke M.C. *Meas. Sci. Technol*., **25**, 035701 (2014).
45. Werncke W., Latka I., Sassning S., Dietzek B., Darvin M.E., Meinke M.C., Popp J., Konig K., Fluhr J.W., Lademann J. *Laser Phys. Lett*., **8**, 895 (2011).
46. Lademann J., Caspers P.J., van der Pol A., Richter H., Patzelt A., Zastrow L., Darvin M., Sterry W., Fluhr J.W. *Laser Phys. Lett*., **6**, 76 (2009).
47. Stamatas G.N., de Sterke J., Hauser M., von Stetten O., van der Pol A. *J. Dermatol. Sci*., **50**, 135 (2008).